Research Article
doi: 10.1590/01047760202531013530
vol(31), 2025

CERNE

Multivariate models based on spectral data for the classification of charcoals produced at different final carbonization temperatures

Michael Douglas Roque Lima[1,2]✤, Amanda Ribeiro de Melo[2], Joabel Raabe[2], Paulo Fernando Trugilho[1], Thiago de Paula Protásio[1], Paulo Ricardo Gherardi Hein[1]

[1]Federal University of Lavras, Department of Forest Sciences, Lavras, MG, Brazil
[2]State University of the Tocantina Region of Maranhão, Agricultural Sciences Center, Department of Forestry Science, Imperatriz, MA, Brazil

TECHNOLOGY OF FOREST PRODUCTS

ABSTRACT

Background: The prediction of apparent relative density (ARD) based on spectral data obtained in the near-infrared (NIR) region has not achieved high accuracy in the literature, emphasizing the need for alternatives to enable the use of NIR technology for classifying charcoal by ARD. In this context, the present study aimed to investigate the precision of NIR in estimating ARD classes for charcoal produced at different carbonization temperatures. Wood wastes from six tropical species (*Dinizia excelsa*, *Licania* sp., *Brosimum gaudichaudii*, *Caryocar* sp., *Simaba guianensis*, and *Parkia* sp.) were carbonized at four final temperatures (400, 500, 600, and 700 °C) under laboratory conditions. The spectral data collected from the radial and transverse surfaces of the charcoals were analyzed using Principal Component Analysis (PCA) and Partial Least Squares Discriminant Analysis (PLS-DA).

Results: While PCA was ineffective in distinguishing the ARD classes, PLS-DA demonstrated relevant accuracy for classification. The quality of the PLS-DA models varied depending on the final carbonization temperature and the surface from which the spectra were collected. Spectral data from the radial and transverse surfaces showed high accuracy in classifying charcoals (>70%) up to 500 °C for ARD. A global model with data from temperatures of 400–500 °C achieved accuracy rates of 74% (transverse) and 80% (radial).

Conclusion: Using NIR technology for ARD classification represents significant progress for the energy sector, especially in the pursuit of bio-reducers with suitable quality for industrial applications.

Keywords: Amazonian wastes; tropical woods; charcoal quality; NIRS; carbonization temperature.

HIGHLIGHTS

NIR spectroscopy distinguished density classes of charcoals from tropical species.
PLS-DA models achieved high accuracy for charcoal classification at 400–500 °C.
Radial and transverse surfaces achieved >70% accuracy for charcoal up to 500 °C.
Global PLS-DA models for 400–500 °C charcoals reached up to 79.6% classification accuracy.

LIMA, M. D. R.; MELO, A. R.; RAABE, J.; TRUGILHO, P. F.; PROTÁSIO, T. P.; HEIN, P. R. G.; Multivariate models based on spectral data for the classification of charcoals produced at different final carbonization temperatures. CERNE, v.31, e-103530, 2025. doi: 10.1590/01047760202531013530

✤Corresponding author: michael.lima1@ufla.br
Scientific Editor: Amélia Guimarães Carvalho

Received: January 22, 2025
Accepted: March 24, 2025

CERNE
ISSN 0104-7760
UNIVERSIDADE FEDERAL DE LAVRAS

INTRODUCTION

Charcoal is a carbonaceous material of great importance for various industrial sectors, especially the steel industry. Brazil leads the global ranking of charcoal producers, with 6.6 million tons produced in 2023, all destined for the domestic market (EPE, 2024). In Brazil, planted forests and residues from the forestry industry have replaced native forests as the primary sources of wood for charcoal production (Silva et al., 2020), driven by increasing environmental demands and sustainability concerns.

It is widely used for domestic purposes as well as fuel in steel production, charcoal plays an indispensable role in pig iron production (Pinto et al., 2018; EPE, 2024). In 2022, the steel and iron sectors produced 7.8 million tons of pig iron using charcoal as raw material (SINDIFER, 2023). Charcoal production occurs through the carbonization of biomass, a thermal decomposition process that takes place under controlled temperature and limited oxygen conditions (Fortaleza et al., 2019). Charcoal quality is often evaluated by its physical and chemical properties, with apparent relative density (ARD) being one of the most relevant parameters. ARD directly influences energy efficiency, storage, and transport capacity, as well as pollutant emissions during combustion (Loureiro et al., 2021).

Traditional methods for determining ARD, such as liquid immersion and pycnometry (Araújo et al., 2018), while precise, are typically time-consuming and destructive, limiting their application in large-scale quality control processes. In this context, alternative techniques that provide rapid and accurate analysis and results are necessary, such as Near Infrared (NIR) Spectroscopy (Lima et al., 2022a). The NIR technique is based on the interaction of near-infrared radiation with matter, resulting in spectra that can be analyzed to extract information about the chemical composition and physical properties of the material. NIR has been extensively used in agriculture (Alves et al. 2024), the food industry, and the pharmaceutical industry for rapid analysis of various product properties, demonstrating its versatility and efficiency (Rech and Werner, 2024).

NIR combined with Partial Least Squares Regression (PLS-R) demonstrated high accuracy in predicting wood properties such as basic density (cross-validation coefficient of determination – $R^2cv > 0.90$) (Medeiros et al., 2023; Nascimento et al., 2017), moisture (R^2cv: 0.96) (Santos et al., 2021), modulus of elasticity (R^2cv: 0.78) and rupture (R^2cv: 0.73) (Schimleck et al., 2018), total extractives (R^2cv: 0.91), ash (R^2cv: 0.96), elemental carbon (R^2cv: 0.76) (Loureiro et al., 2022), Klason lignin (R^2cv: 0.86), acid-soluble lignin (R^2cv: 0.77), syringyl/guaiacyl ratio (R^2cv: 0.86) (Hein et al., 2010), volatile materials (R^2cv: 0.99), fixed carbon (R^2cv: 0.99), and higher heating value (R^2cv: 0.98) (Gmach et al., 2024).

For charcoal, PLS-R models based on spectral data have accurately estimated volatile materials (R^2cv: 0.87), fixed carbon (R^2cv: 0.88), and higher heating value (R^2cv: 0.86) (Gomes et al., 2024). However, Costa et al. (2018) attempted to adjust ARD prediction models using PLS-R and observed weak correlations between actual and predicted values. The reasons for NIR's inability to predict charcoal ARD remain unclear. The literature lacks detailed information explaining the behavior of prediction models for ARD in charcoals from wood wastes. An alternative approach is to calibrate multivariate models using NIR spectral data with the Partial Least Squares Discriminant Analysis (PLS-DA) technique to estimate ARD classes proposed by Lima et al. (2022a). These authors proposed three ARD classes for charcoal derived from wood wastes for steelmaking purposes: Class 1 ($0.250 \leq ARD < 0.400$ g cm^{-3}), Class 2 ($0.400 \leq ARD < 0.550$ g cm^{-3}), and Class 3 ($ARD \geq 0.550$ g cm^{-3}).

This research topic is justified by the need for more efficient methods to analyze charcoal quality, aiming to optimize industrial processes and promote sustainability. Thus, this study contributes to advancing scientific knowledge in the field of lignocellulosic material analysis and offers practical implications for the charcoal industry, enabling improvements in production and quality control processes. The scientific questions guiding this study were: i) What is the accuracy of multivariate statistical models calibrated with NIR spectra for classifying charcoal from wood wastes into ARD classes? ii) Is the accuracy of predictive models influenced by the final carbonization temperature? iii) What is the optimal ARD range for accurately classifying charcoals? Accordingly, the study aimed to investigate the precision of NIR in estimating ARD classes for charcoal produced at different carbonization temperatures.

MATERIAL AND METHODS

Origin of the wood wastes

The wood wastes were collected at the storage yard of the charcoal production unit of Rio Capim Farm (coordinates: 3º 30′ and 3º 45′S – 48º 30′ and 48º 45′W; altitude around 87 m), located in Paragominas town, Pará State, Brazil. This plant belongs to the Keilla group and operates under a license issued by the Secretariat of Environment and Sustainability of the state of Pará (SEMAS – PA).

Sampling and botanical identification of wastes

Six different tropical species (Table 1) were selected for this study based on the apparent relative density (ARD) values of the charcoal produced at 400 °C and the ARD classes proposed by Lima et al. (2022a). The following classes were considered for species selection: Class 1 ($0.250 \leq ARD < 0.400$ g cm^{-3}), Class 2 ($0.400 \leq ARD < 0.550$ g cm^{-3}), and Class 3 ($ARD \geq 0.550$ g cm^{-3}). The species were also selected for their widespread use in the charcoal production unit and their high availability of wastes in the storage yard, ensuring the reproducibility of the study.

In the storage yard, species were identified and labeled in the waste piles with the assistance of a botanical identifier. Subsequently, these waste pieces were removed using a Wheel Loader (Volvo L90 F) and sectioned into six short logs, each 60 cm in length, by a chainsaw operator. From each short logs, a 20 cm-thick wood disc was extracted for laboratory carbonization and spectral readings.

From the 20 cm-thick wood discs, 72 defect-free specimens (4 x 4 x 3 cm) per species were prepared for laboratory-scale carbonization, analysis of the apparent relative density (ARD), and anatomical identification in the xylotheque of Embrapa Eastern Amazon (Lima et al., 2022a). The sampling methodology aimed to isolate intraspecific variations in charcoal properties, ensuring that only the effects of final carbonization temperature were observed and evaluated for multivariate models based on the charcoal spectral data. Figure 1 illustrates the sampling methodology for laboratory carbonization and analysis of the produced charcoals.

Laboratory-scale carbonization

Laboratory carbonizations were performed using an electric muffle furnace (model Q318S25T, Quimis, São Paulo, Brazil). The equipment included a carbonization capsule connected to a water-cooled condenser coupled with a volatile gas collection flask.

A total of 72 wood specimens per species were carbonized in the laboratory. For each final carbonization temperature (400, 500, 600, and 700 °C), 18 samples per species were used, simulating the temperature variations found in real conditions in brick kilns. Before carbonization,

Table 1: Selected tropical species for the study.

Scientific Name	Family	Common Name	ARD (g cm^{-3})	Class
Licania sp.	Chrysobalanaceae	Casca-seca	0.642 ± 0.050	3
Dinizia excelsa Ducke	Fabaceae	Angelim-vermelho	0.617 ± 0.031	3
Brosimum gaudichaudii Trécul	Moraceae	Inharé	0.455 ± 0.016	2
Caryocar sp.	Caryocaraceae	Pequiarana	0.404 ± 0.040	2
Parkia sp.	Fabaceae	Fava-branca	0.322 ± 0.042	1
Simaba guianensis (Aubl.) Engl.	Simaroubaceae	Marupá-amarelo	0.283 ± 0.028	1

ARD = apparent relative density of charcoal. Source: Lima et al. (2022a).

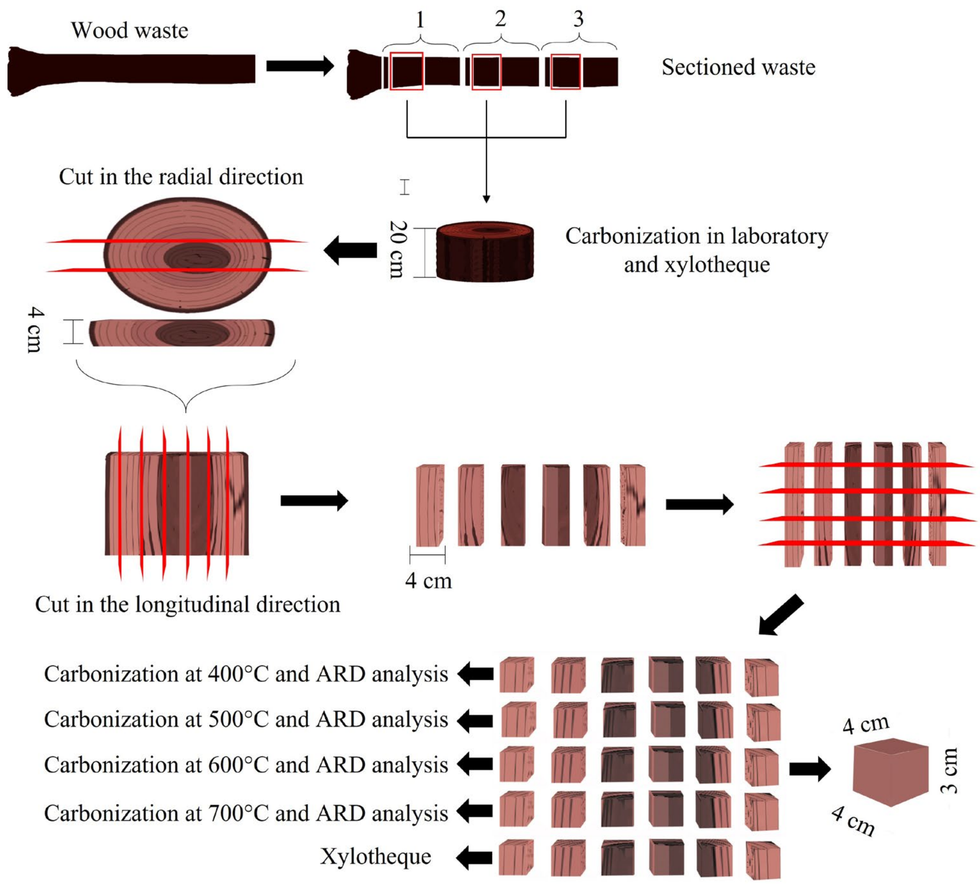

Figure 1: Sampling scheme for wood wastes aimed at laboratory-scale carbonization at different final temperatures and analysis of the apparent relative density (ARD) of the charcoal.

the specimens were dried in an oven with forced air circulation (105 ± 2 °C for 24 hours). Carbonization began at an initial temperature of 100 °C, with a heating rate of 1.67 °C/min and a residence time of 60 minutes at the final temperature, following a methodology adapted from Trugilho et al. (1991).

Determination and classification of charcoals based on apparent relative density (ARD)

The apparent relative density (ARD) of the charcoal was determined following an adaptation of the NBR 11941 standard (ABNT, 2003), using the hydrostatic method to measure the saturated volume of the sample. The adaptations included a 30-minute immersion time for the charcoal sample and a drying period in an oven with air circulation (105 ± 2 °C for 2 hours).

The charcoals were classified into ARD classes as proposed by Lima et al. (2022a): Class 1 (0.250 ≤ ARD < 0.400 g cm^{-3}), Class 2 (0.400 ≤ ARD < 0.550 g cm^{-3}), and Class 3 (ARD ≥ 0.550 g cm^{-3}). Charcoals with ARD values below 0.250 g cm^{-3} were excluded from the dataset used to adjust the multivariate models described later. This classification was employed due to the absence of established technical standards. Additionally, the literature suggests that, for industrial purposes, charcoals with ARD ≥ 0.250 g cm^{-3} are suitable as they exhibit higher mechanical strength (Assis et al., 2016), supporting the coherence and applicability of the adopted classification.

NIR Spectra acquisition

Spectral readings were conducted on laboratory-produced charcoal samples, totaling 432 specimens. The readings were performed in diffuse reflectance mode using a Fourier-transform spectrometer (model MPA, Bruker Optik GmbH, Ettlingen, Germany) equipped with an integrating sphere and an optical fiber. The spectral data were acquired using OPUS software version 7.5, covering the radiation range of 3,500–12,500 cm^{-1} with a resolution of 8 cm^{-1} via the integrating sphere. However, only the 4,000–9,000 cm^{-1} range was considered due to noise and lack of relevant information in the excluded range (Santos et al., 2021). Average spectral curves for each ARD class, considering the acquisition surfaces (radial and transverse), were analyzed to observe changes due to temperatures. The number of spectra collected is described in Table 2.

Multivariate statistical analysis

Principal Component Analysis (PCA) and Partial Least Squares Discriminant Analysis (PLS-DA) were conducted using Chemoface software version 1.66 (Nunes et al., 2012). PCA was performed to preliminarily explore data dependency and verify spectral similarity among the obtained data. Models were validated using the cross-validation method (leave-one-out). The number of latent variables was determined based on the lowest root mean square error of prediction (RMSEP) and the highest coefficient of determination for validation (R^2cv).

PLS-DA was employed to develop models for classifying charcoal into ARD classes as proposed by Lima et al. (2022a): Class 1 (0.250 ≤ ARD < 0.400 g cm^{-3}), Class 2 (0.400 ≤ ARD < 0.550 g cm^{-3}), and Class 3 (ARD ≥ 0.550 g cm^{-3}). This method, based on the PLS-R approach, correlates two blocks of variables: X (independent variables) and Y (dependent variables). The independent variables (X) were represented by the NIR spectral matrix, while the dependent variables (Y) corresponded to the ARD classes. Models were adjusted using spectral data treated with the first and second derivatives and untreated data. Outliers were identified through graphical analysis of residuals. Additionally, spectra from charcoals with ARD below 0.250 g cm^{-3} were excluded.

PLS-DA models were calibrated and validated using the leave-one-out cross-validation method. Finally, a confusion matrix was constructed to analyze the percentages of errors and correct classifications after testing the model generated by PLS-DA. Global models, encompassing data from different temperature ranges (400–700 °C; 400–600 °C; and 400–500 °C), were adjusted to simulate the carbonization temperature ranges of brick kilns in the Brazilian Amazonia.

Table 2: Number of NIR spectral readings, considering final carbonization temperatures, spectral acquisition surfaces, and ARD classes.

Temperature	Surface	ARD Classes			Total spectral readings
		1	2	3	
400	Radial	40	28	36	104
	Transverse	40	28	36	104
500	Radial	45	27	34	106
	Transverse	45	27	34	106
600	Radial	41	31	31	103
	Transverse	41	31	31	103
700	Radial	36	34	37	107
	Transverse	36	34	37	107
Total	-	324	240	276	840

ARD = Apparent relative density of charcoal.

RESULTS

The mean ARD values of charcoal produced from wood wastes of six tropical species are shown in Figure 2. The charcoals from *Licania* sp. and *D. excelsa* exhibited the highest ARD values and were classified in Class 3 across all final carbonization temperatures. *B. gaudichaudii* and *Caryocar* sp. consistently represented Class 2 at different carbonization temperatures, while *Parkia* sp. and *S. guianensis* were always classified in Class 1. Although no transitions between classes occurred during carbonization, slight modifications in ARD values were observed with increasing temperature: between 400–500 °C (-1.9%), 500–600 °C (0.5%), and 600–700 °C (7.9%).

Figure 3 highlights the behavior of spectral signatures for the radial (a, b, and c) and transverse (d, e, and f) surfaces as a function of final carbonization temperatures and ARD classes. The spectral curves exhibit an ascending trend up to 600 °C, with the 400 °C temperature positioned in the lower region of the plot. The 700 °C curve overlaps with the others. As ARD increases, the curves become closer to each other, indicating a lower amplitude of NIR absorbance on both data collection surfaces. A small absorbance peak was observed only at 400 °C between 5,500 and 5,000 cm^{-1}.

The PCA scores demonstrated the spectral variability of charcoal surfaces produced at different carbonization temperatures. Figures 4 and 5 depict the spectral data obtained from radial and transverse surfaces, respectively. Although PCA did not clearly separate ARD classes, trends of point clustering within the same class were evident in Figures 4c (raw radial surface data for charcoal produced at 500 °C), 4d (first derivative data from the radial surface at 500 °C), 5b (first derivative transverse surface data at 400 °C), and 5c (raw transverse surface data at 500 °C).

Table 3 summarizes the accuracy achieved by PLS-DA models in predicting ARD classes for charcoals produced at specific carbonization temperatures. At 400 °C, the PLS-DA model adjusted with raw spectral data from the transverse surface demonstrated the highest accuracy (81.44%). When the temperature increased to 500 °C, radial surface data exhibited significantly improved classification accuracy (86.43%). Models for carbonized charcoals at 600 °C achieved accuracies around 70.10%, with a subsequent decline to approximately 68.90% at 700 °C.

The confusion matrix for the model adjusted with raw spectral data from the transverse surface at 400 °C revealed that 87 samples were correctly classified, resulting in an accuracy rate of 81.44%. Class 1 demonstrated excellent performance, with 97.50% of samples correctly classified, while Class 2 had the lowest accuracy (60.71%).

At 500 °C, the radial surface model correctly classified 94 charcoal samples. Classes 1 and 3 demonstrated the highest accuracies, while Class 2 presented greater challenges, with nine samples misclassified (Table 5).

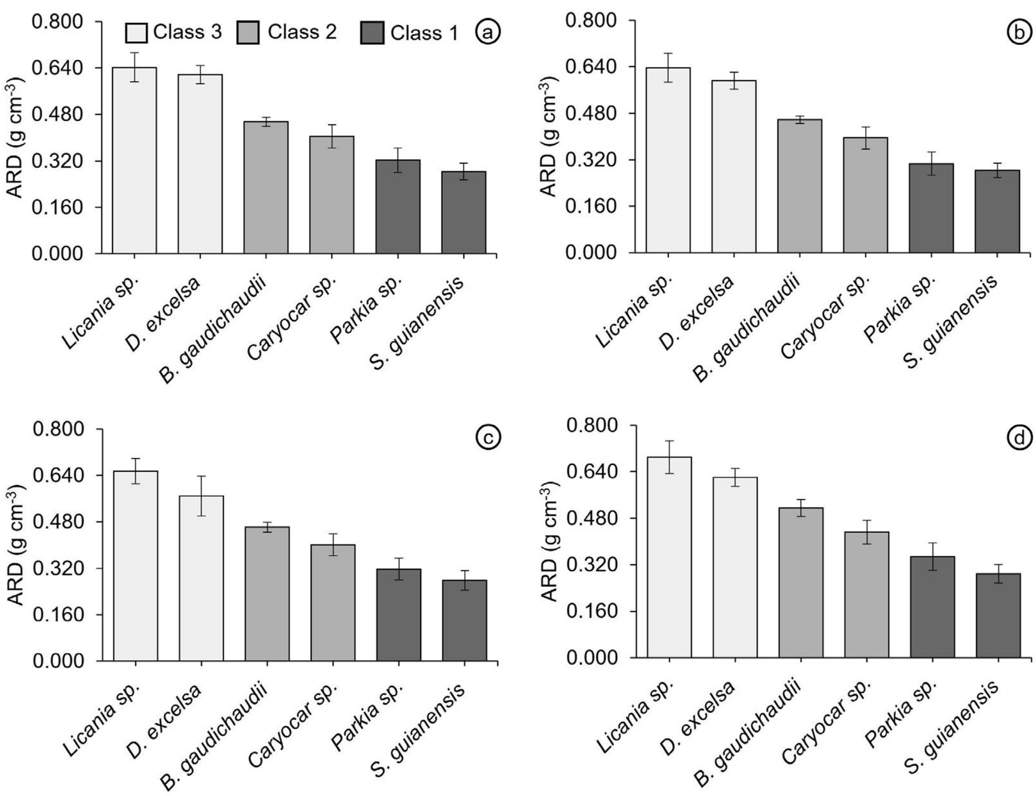

Figure 2: Apparent relative density (ARD) of charcoals from Amazonian wood wastes produced at final carbonization temperatures of 400 (a), 500 (b), 600 (c), and 700 °C (d). The bar colors differentiate from the ARD classes proposed by Lima et al. (2022a), and the error bars represent the standard deviation.

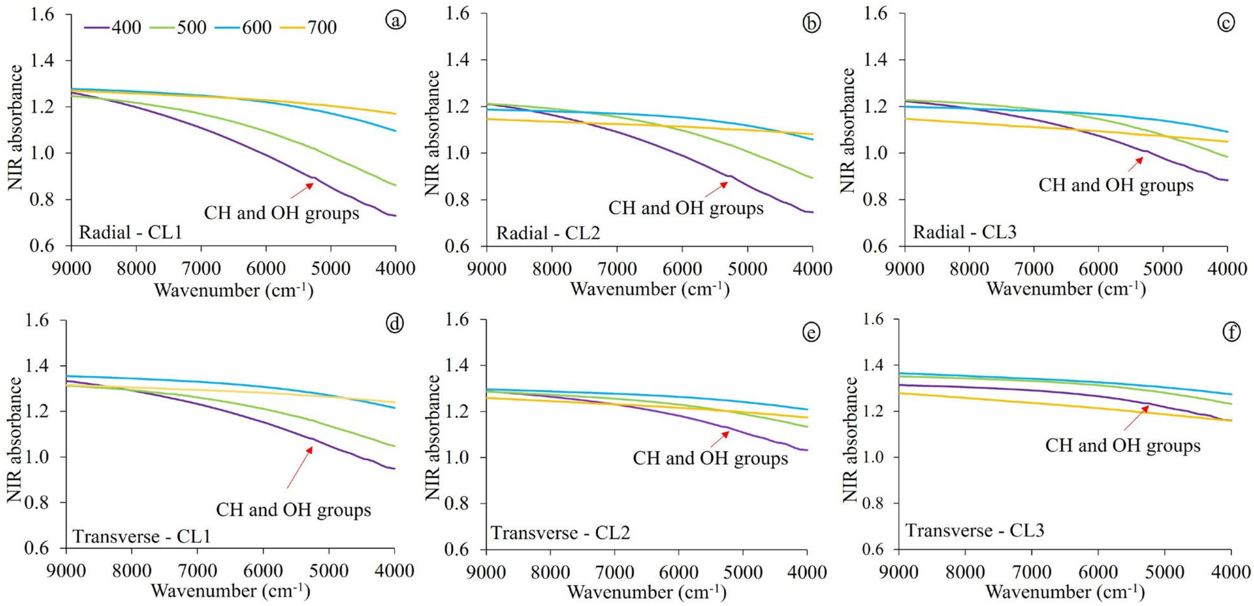

Figure 3: Average spectra collected from the radial (a, b, and c) and transverse (d, e, and f) surfaces, showing twelve ARD classes categorized by final carbonization temperature. CL1, CL2, and CL3: ARD classes 1, 2, and 3. 400, 500, 600, and 700ºC: final carbonization temperatures.

Global PLS-DA models considering the 400–500 °C temperature range demonstrated the highest classification accuracy for ARD classes, achieving 79.59% accuracy for radial surfaces and 74.01% for transverse surfaces (Table 6). In contrast, models encompassing wider temperature ranges (400–600 °C and 400–700 °C) showed reduced precision, even with mathematical treatment of the data, with classification accuracies below 65%.

The confusion matrix for the global PLS-DA model adjusted with raw spectral data from charcoals produced in the 400–500 °C range revealed that 172 samples were correctly classified, yielding an accuracy rate of 79.59%. The model struggled most with distinguishing between Classes 2 and 3 (Table 7). Class 1 performed well, with 90.59% of samples correctly classified, whereas Class 2 had the lowest accuracy (58.18%).

DISCUSSION

Apparent relative density of charcoals from wood wastes

The ARD of the evaluated charcoals was minimally influenced by the final carbonization temperature. This result is thoroughly analyzed in the study by Lima et al. (2022a), who used a quadratic polynomial regression curve to represent the relationship between ARD and final carbonization temperature. The authors emphasized that the species factor has a more significant influence on the ARD of charcoal derived from Amazonian residual wood than the final carbonization temperature.

The reduction in DRA between 400 and 600 ºC is due to the release of volatile gases from the degradation of carbohydrates in the woody cell wall and the increase in the charcoal's porosity (Costa et al., 2017). Above 600 ºC, the release of volatiles decreases, and an anatomical change occurs, with alterations in the material's vessels and an increase in the fiber ratio (Trugilho and Silva, 2001). Additionally, there is a structural rearrangement of the charcoal's components, particularly the carbon, forming more resistant structures like graphite (Couto et al., 2015), which explains the increase in CAD at 700 ºC.

The literature demonstrates that ARD is strongly influenced by the wood's basic density, with denser woods resulting in denser charcoal (Santos et al., 2023). It is worth noting that both anatomical (lumen diameter, vessel density, wall fraction, and cell wall thickness) and physical (basic density) characteristics of the wood influence the charcoal's ARD (Couto et al., 2023; Silva et al., 2024), which may explain the variations in this characteristic observed in the present study (see Figure 2). In our study, the species *Licania* sp. and *D. excelsa* exhibited higher ARD values at all final carbonization temperatures, which can be justified by the higher basic densities of their woods (0.927 and 0.881 g cm^{-3}), as described by Lima et al. (2022b).

The ARD ranges provide an alternative for classifying charcoals for steelmaking purposes, encompassing ARD values starting from 0.250 g cm^{-3} (Assis et al., 2016). This reference includes charcoals with higher mechanical resistance, which enhances their ability to support the weight of iron ore and increases the internal utilization of charcoal within blast furnaces. Hence, the studied charcoals are suitable for industrial applications and can supply the Carajás steelmaking complex in Amazonia, complementing the charcoal produced from *Eucalyptus* sp. cultivated in emerging energy forests.

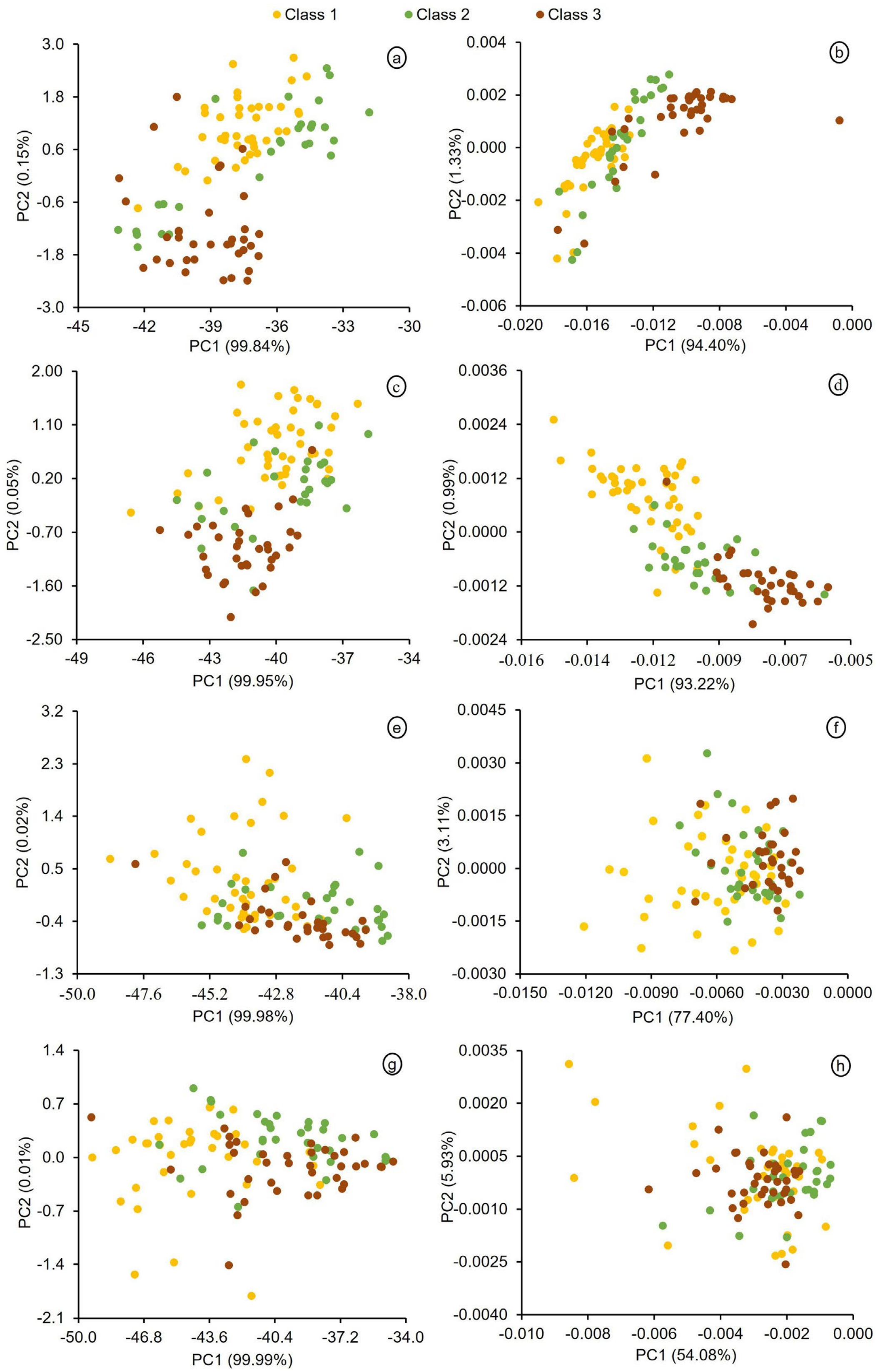

Figure 4: Scores of the principal component analysis of untreated (a, c, e, and f) and first derivative-treated (b, d, f, and h) spectral data, obtained on the radial surface of charcoals classified into 3 DRA classes and produced at final carbonization temperatures of 400 (a and b), 500 (c and d), 600 (e and f), and 700 (g and h) °C.

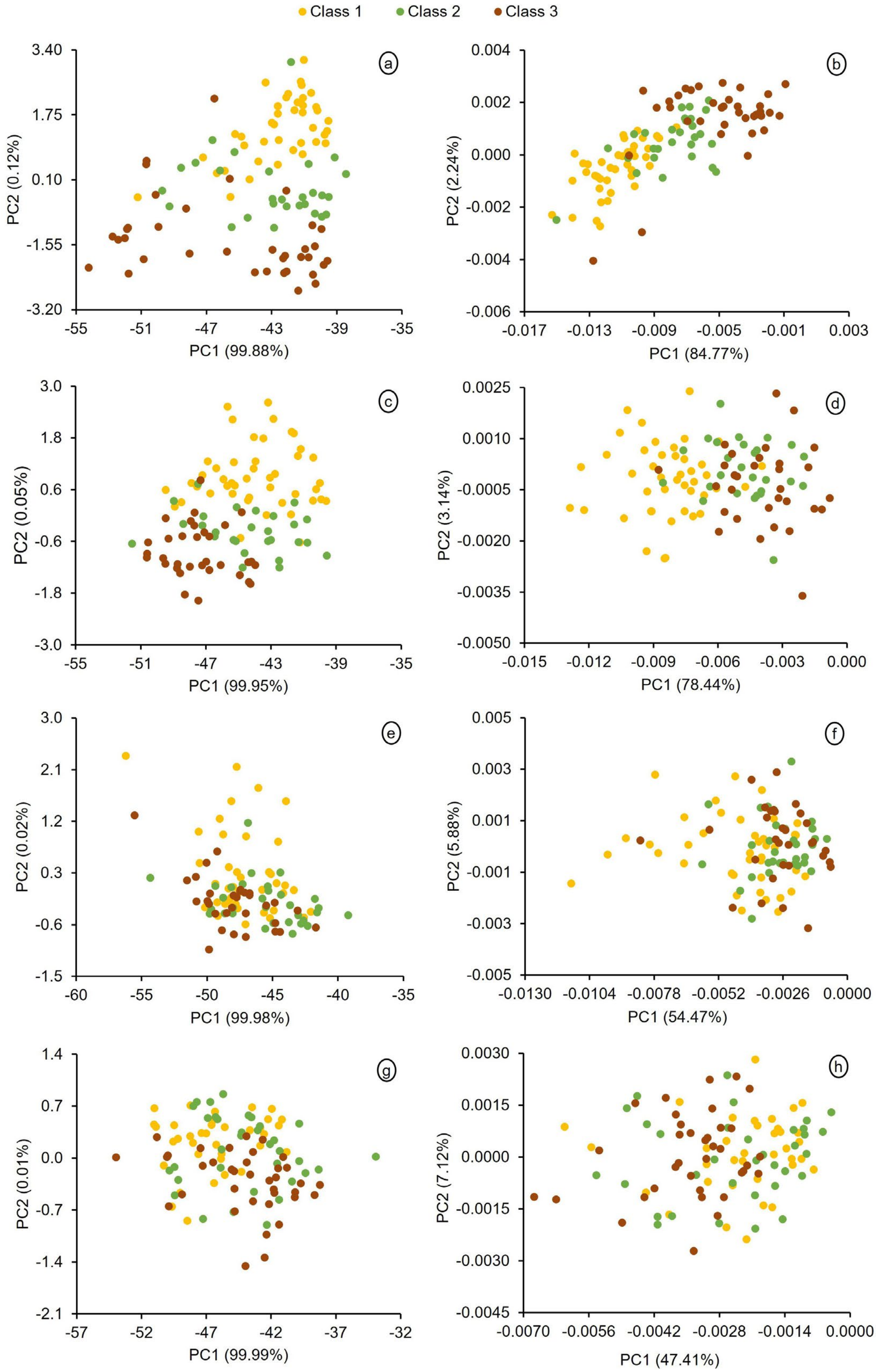

Figure 5: Scores of the principal component analysis of untreated (a, c, e, and f) and first derivative-treated (b, d, f, and h) spectral data, obtained on the transverse surface of charcoals classified in 3 DRA classes and produced at final carbonization temperatures of 400 (a and b), 500 (c and d), 600 (e and f), and 700 (g and h) °C.

Table 3: Accuracy summary for charcoal classification using PLS-DA with cross-validation, stratified by carbonization temperature, spectral acquisition surface, and mathematical pre-treatments.

400 ºC												
	Radial						**Transverse**					
	WT (10 LV)		**1d (10 LV)**		**2d (6 LV)**		**WT (7 LV)**		**1d (2 LV)**		**2d (8 LV)**	
Classes	n	%	n	%	n	%	n	%	n	%	n	%
1	35	87.50	36	90.00	21	52.50	39	97.50	40	100.00	19	47.50
2	17	60.71	19	67.86	10	35.71	17	60.71	0	0.00	10	35.71
3	26	72.22	26	72.22	18	50.00	31	86.11	30	83.33	13	36.11
Average	-	73.48	-	76.69	-	46.07	-	81.44	-	61.11	-	39.78
500 ºC												
	Radial						**Transverse**					
	WT (5 LV)		**1d (4 LV)**		**2d (4 LV)**		**WT (5 LV)**		**1d (2 LV)**		**2d (2 LV)**	
Classes	n	%	n	%	n	%	n	%	n	%	n	%
1	43	95.56	42	93.33	42	93.33	45	100.00	45	100.00	43	95.56
2	18	66.67	18	66.67	15	55.56	12	44.44	0	0.00	4	14.81
3	33	97.06	28	82.35	24	70.59	30	88.24	32	94.12	17	50.00
Average	-	86.43	-	80.78	-	73.16	-	77.56	-	64.71	-	53.46
600 ºC												
	Radial						**Transverse**					
	WT (7 LV)		**1d (6 LV)**		**2d (6 LV)**		**WT (3 LV)**		**1d (2 LV)**		**2d (8 LV)**	
Classes	N	%	n	%	n	%	n	%	n	%	n	%
1	32	78.05	26	63.41	19	46.34	27	65.85	32	78.05	19	46.34
2	17	54.84	20	64.52	15	48.39	13	41.94	9	29.03	12	38.71
3	24	77.42	16	51.61	17	54.84	24	77.42	15	48.39	8	25.81
Average	-	70.10	-	59.85	-	49.86	-	61.74	-	51.82	-	36.95
700 ºC												
	Radial						**Transverse**					
	WT (5 LV)		**1d (2 LV)**		**2d (2 LV)**		**WT (7 LV)**		**1d (6 LV)**		**2d (5 LV)**	
Classes	n	%	n	%	n	%	n	%	n	%	n	%
1	29	80.56	16	44.44	15	41.67	20	55.56	20	55.56	13	36.11
2	19	55.88	17	50.00	10	29.41	14	41.18	17	50.00	13	38.24
3	26	70.27	29	78.38	19	51.35	28	75.68	22	59.46	13	35.14
Average	-	68.90	-	57.61	-	40.81	-	57.47	-	55.01	-	36.49

LV = Latent variable; WT = without treatment; 1d = first derivative (15x2x1); 2d = second derivative (15x2x2).

Table 4: Confusion matrix for charcoal classification using PLS-DA with cross-validation and untreated spectral data from the transverse surface at 400 °C.

Classes	**NIR predicted classification (7 LVs)**				
	1	2	3	n	(%)
1	39	0	1	39	97.50
2	5	17	6	17	60.71
3	1	4	31	31	86.11
General classification				87	81.44

LVs = latent variables.

NIR spectra of charcoal

The increase in carbonization temperature results in greater homogeneity in the physical and chemical structure of charcoal (Lima et al., 2022a). This is particularly evident in charcoals produced at 700 °C, where the chemical structure becomes more uniform, reducing spectral differences between ARD classes. This homogenization may be associated with the stabilization of the carbonaceous matrix, the elimination of volatile functional groups, and the structural reorganization of the remaining compounds (Machado et al., 2014; Oliveira et al., 2020).

The lower amplitude of NIR absorbance on both surfaces in denser charcoals suggests that ARD influences the spectral response, making distinctions between classes less evident at higher temperatures. This highlights the importance of strict control of the carbonization process, especially the final carbonization temperature, to ensure the predictability of charcoal properties and their industrial applications.

Table 5: Confusion matrix for charcoal classification using PLS-DA with cross-validation and untreated spectral data from the radial surface at 500 °C.

Classes	NIR predicted classification (7 LVs)				
	1	2	3	n	(%)
1	43	2	0	43	95.56
2	6	18	3	18	66.67
3	1	0	33	33	97.06
General classification				94	86.43

LVs = latent variables.

Spectral curves at 400 °C, on both the radial and transverse surfaces, revealed prominent absorption peaks between 5,000–6,000 cm^{-1}. This pattern reflects the degradation of polymers in the original material, such as lignin, cellulose, and hemicelluloses, during carbonization (Muñiz et al., 2013). At this stage, the primary functional groups detected were OH and CH. As the final carbonization temperature increased to 700 °C, these peaks weakened or disappeared, indicating the loss of these functional groups (Dias Junior et al., 2019). This reduction is associated with increased carbon content and decreased hydrogen-to-carbon (H/C) and oxygen-to-carbon (O/C) ratios, suggesting a transition toward a more stable carbon structure with fewer functional groups (Liu et al., 2018). These changes are primarily driven by demethanation, dehydration, and decarboxylation reactions, which become more pronounced at higher temperatures (Wu et al., 2018).

Jo et al. (2009) observed that higher carbonization temperatures increase the proportion of C-C bonds while significantly reducing C-O-H bonds. Chemical bonds involving oxygen tend to break, resulting in greater stability and higher carbon content in the material (Liu et al., 2018). During carbonization, chemical bonds undergo partial decomposition, formation, and recombination stages, justifying the reduction in chemical functional groups (Jo et al., 2009).

Regarding ARD behavior, charcoals at 600 °C and 700 °C exhibited greater homogeneity due to the loss of functional groups, which was reflected in the average spectral curves for ARD classes at these temperatures. However, visual analysis based on these spectral signatures did not allow for clear classification of the ARD values. Therefore, PCA was applied to enhance the distinction between ARD classes, providing a statistical approach to identify groups with similar characteristics.

Table 6: Accuracy summary of global PLS-DA models calibrated with spectral data from charcoals produced at different temperature ranges (400–700 °C, 400–600 °C, and 400–500 °C), using cross-validation and considering spectral acquisition surfaces and applied pre-treatments.

400 – 700 ºC												
	Radial						Transverse					
Classes	WT (5 LV)		1d (8 LV)		2d (8 LV)		WT (7 LV)		1d (2 LV)		2d (4 LV)	
	n	%	n	%	n	%	n	%	n	%	n	%
1	136	83.95	102	62.96	85	52.47	106	65.43	110	67.90	92	56.79
2	26	21.67	41	34.17	25	20.83	52	43.33	0	0.00	41	34.17
3	90	65.22	76	55.07	69	50.00	71	51.45	100	72.46	46	33.33
Average	-	56.94	-	50.73	-	41.10	-	53.40	-	46.79	-	41.43
400 – 600 ºC												
	Radial						Transverse					
Classe	ST (8 LV)		1d (7 LV)		2d (8 LV)		ST (7 LV)		1d (2 LV)		2d (2 LV)	
	n	%	n	%	n	%	n	%	n	%	n	%
1	104	82.54	88	69.84	85	67.46	95	75.40	104	82.54	78	61.90
2	30	34.88	24	27.91	5	5.81	38	44.19	0	0.00	24	27.91
3	76	75.25	73	72.28	58	57.43	68	67.33	80	79.21	42	41.58
Average	-	64.22	-	56.68	-	43.57	-	62.30	-	53.92	-	43.80
400 – 500 ºC												
	Radial						Transverse					
Classe	ST (5 LV)		1d (5 LV)		2d (2 LV)		ST (8 LV)		1d (2 LV)		2d (2 LV)	
	n	%	n	%	n	%	n	%	n	%	n	%
1	77	90.59	75	88.24	61	71.76	79	92.94	84	98.82	61	71.76
2	32	58.18	31	56.36	19	34.55	27	49.09	0	0.00	11	20.00
3	63	90.00	59	84.29	42	60.00	56	80.00	62	88.57	31	44.29
Average	-	79.59	-	76.29	-	55.44	-	74.01	-	62.46	-	45.35

LV = Latent variable; WT = without treatment; 1d = first derivative (15x2x1); 2d = second derivative (15x2x2).

Table 7: Confusion matrix for ARD classification using global PLS-DA models and untreated spectral data from radial surface of charcoals produced at 400–500 °C.

Classes	NIR predicted classification (5 LVs)				
	1	2	3	n	(%)
1	77	8	0	77	90.59
2	17	32	6	32	58.18
3	7	0	63	63	90.00
General classification				172	79.59

LVs = Latent variables.

Principal Component Analysis (PCA)

These figures reveal important ARD patterns, highlighting a clear directional growth in this variable as indicated by the PCA scores. Overall, spectral data without mathematical treatments resulted in a higher percentage of explained cumulative variance for the principal components across all temperatures and collection surfaces.

While PCA applied to both untreated and first derivative data provided insight into ARD growth trends, it was insufficient for clearly distinguishing charcoal density classes due to significant overlap of points among classes. This limitation may be attributed to the homogeneous structure of charcoal, which resembles graphite (Couto et al., 2015). The authors noted that increasing carbonization temperatures result in significant structural rearrangements in charcoal, particularly in its carbon chains.

In this study, as carbonization temperature increased, segregation between ARD classes became more challenging, with greater score overlap observed. Costa et al. (2019) similarly reported that PCA could not differentiate species based on spectral data collected from charcoals. They suggested that NIR spectral analysis using PLS-DA is a promising solution for classifying charcoal samples, as it achieved high accuracy in classifying charcoals based on fixed carbon content.

Charcoal classification based on PLS-DA models

The results underscore the relevance of NIR spectroscopy for classifying charcoals into ARD classes. Both radial and transverse surfaces achieved high classification accuracies (>70%) for carbonization temperatures up to 500 °C. Beyond this threshold, the radial surface proved more suitable for maintaining classification precision.

Challenges in classifying charcoals at 600 °C and 700 °C may arise from structural changes during carbonization, including carbon stabilization and volatilization of OH and CH functional groups, which negatively impacted the PLS-DA models' ability to differentiate samples. These findings highlight the need for rigorous control of the carbonization process in operational conditions, especially in the Amazon region, where empirical practices based on carbonizer subjectivity are predominant (Lima et al., 2020, 2022a).

The carbonization conducted under operational conditions with standardized final temperatures of 400 and 500 °C can result in better productivity rates for brick kilns and higher gravimetric yield of charcoal, in addition to a shorter carbonization cycle (Lima et al., 2023). This improvement can positively impact the number of monthly carbonizations, production, and revenues generated by the plant, suggesting lower resource immobilization and a faster recovery of the invested capital. Lima et al. (2022a) demonstrated that this optimized temperature range reduces the specific consumption of firewood and maintains the appropriate ARD of the charcoal, contributing to better performance in the carbonization process of wood wastes produced in Brazilian Amazonia.

Carbonization temperatures of 400 and 500 °C yielded PLS-DA models with the highest accuracies. Confusion matrices were constructed to verify the models' correct and incorrect sample classifications.

The results reported in Tables 4 and 5 indicate that PLS-DA faces significant challenges in correctly classifying charcoals belonging to Class 2. Due to being an intermediate ARD class and having a homogeneous physical and chemical structure, the spectral data of these charcoals overlapped with those of the other two classes (see Fig. 4), which was reflected in the PLS-DA analysis. However, the study presents promising models with a high average accuracy of 81.44% (transverse surface) and 86.43% (radial surface) for the classification of charcoals produced at 400 and 500 °C, respectively. The inclusion of spectral data from the mid-infrared region (Mid-IR: 400–4,000 cm^{-1}) could enhance the classification accuracy of the PLS-DA models, as this region of the spectrum may provide better insights into the structural properties of charcoals derived from residual Amazonian wood.

Overall, the results demonstrated that data from the radial surface were slightly more accurate than those from the transverse surface. However, both surfaces proved effective for predicting charcoal classes based on ARD, as also evidenced by the studies of Costa et al. (2018).

Global models based on carbonization temperatures

The lower accuracy observed in global models for the broader temperature ranges (400–700 °C and 400–600 °C) highlights the urgent need to improve the control of brick kilns to enhance the quality of produced charcoal. The lack of precise control results in greater heterogeneity in the carbonization process, which negatively impacts the quality of pig iron produced in the steel industry. A broad range of final carbonization temperatures reduces the homogeneity of bio-reducers, undermining their industrial applications.

Lima et al. (2022a) investigated the effects of carbonization temperatures on charcoal production from wood wastes sourced from sustainable forest management in Amazonia. The authors observed that increasing carbonization temperatures from 400 °C to 700 °C significantly reduced charcoal gravimetric yield while increasing specific consumption of firewood. They recommended carbonization at 400–500 °C in brick kilns for these wastes to optimize gravimetric yield and ARD.

Costa et al. (2018) used chemometric models (PLS-R and PLS-DA) to estimate charcoal gravimetric yield, ARD, and final carbonization temperatures (400, 500, 600, and 700 °C) of charcoal from eucalypt wood using NIR spectral data. Their results showed over 97% accuracy in predicting final carbonization temperatures with PLS-DA models. However, their PLS-R model failed to provide satisfactory ARD predictions, corroborating the promising potential of ARD classes as an alternative for industrial applications in the steel sector.

The global PLS-DA model (Table 7) struggles with separating Classes 2 and 3, likely due to overlapping spectral characteristics within this temperature range. Incorporating mid-infrared (Mid-IR) spectra could further enhance the accuracy of ARD classification by providing additional structural insights into Amazonian wood charcoals. However, the model demonstrated a high accuracy rate, showcasing the sensitivity of NIR in separating charcoals into ARD classes.

The findings of this study highlight the need for better temperature control during the carbonization process, as the global model adjusted with spectral data from charcoals produced at 400–500 °C exhibited the best predicted classification performance. In this temperature range, the primary functional groups (OH and CH) are better preserved, while at higher carbonization temperatures (600 °C and 700 °C), these functional groups are lost (Dias Junior et al., 2019). These findings emphasize the importance of maintaining the temperature within the 400 °C to 500 °C range to optimize spectral characteristics and ensure improved performance in charcoal classification.

CONCLUSIONS

This study revealed that PCA was ineffective in distinguishing ARD classes of charcoal. The quality of PLS-DA models varied according to the final carbonization temperature and the surface from which spectra were collected, underscoring the importance of rigorous process control.

The PLS-DA model, adjusted with data from the transverse surface of the charcoal at 400 °C, estimated the DRA class with an accuracy of 81.44%. At 500 °C, classification accuracy improved to 86.43% when using data from the radial surface. Beyond this temperature, the radial surface (600 °C = 70.10% and 700 °C = 68.90%) proved to be more suitable for maintaining classification accuracy compared to the transverse surface (600 °C = 61.74% and 700 °C = 57.47%).

The global model, adjusted to estimate the ARD class using spectral data from charcoals produced at temperatures between 400–500 °C, achieved the highest accuracy for the radial (79.59%) and transverse (74.01%) surfaces.

The use of NIR in classifying charcoals by ARD represents significant progress for the sector, particularly in the pursuit of bio-reducers with suitable quality for industrial purposes. Future studies should evaluate the accuracy of portable NIR devices for real-time ARD classification under operational conditions. Additionally, integrating spectral data from the mid-infrared (Mid-IR) region with NIR data should be explored to enhance model performance and broaden the understanding of Amazonian wood charcoal structures.

ACKNOWLEDGEMENTS

This work was supported by the Brazilian National Council for Scientific and Technological Development (CNPq: grants no. 406593/2021-3, 406053/2022-7, 350017/2023-9, 306793/2019–9, 304165/2022-0, and 309620/2020-1), the Coordination for the Improvement of Higher Education Personnel (CAPES - Finance Code 001), the Minas Gerais State Research Support Foundation (FAPEMIG: APQ-00742-23 and APQ-05431-24), Banco da Amazônia (financial support contract nº. 2018/193), Keilla Group, Multiuser Laboratory of Biomaterials and Biomass Energy of the Federal University of Lavras (UFLA, Brazil), and Laboratory of Wood Anatomy and Technology of the State University of the Tocantina Region of Maranhão (UEMASUL, Brazil).

AUTHORS' CONTRIBUTION

Project Idea: M. D. R. L.; T. P. P.; P. R. G. H.

Funding: P. F. T.; T. P. P.; P. R. G. H.

Database: M. D. R. L.; A. R. M.; T. P. P.; P. R. G.H.

Processing: M. D. R. L.; A. R. M.; T. P. P.; P. R. G. H.

Analysis: M. D. R. L.; A. R. M.; T. P. P.; P. R. G. H.

Writing: M. D. R.L.; A. R. M.; J. R.; P. F. T.; T. P. P.; P. R. G. H.

Review: M. D. R. L.; A. R. M.; J. R.; P. F. T.; T. P. P.; P. R. G. H.

REFERENCES

ABNT – Associação Brasileira de Normas Técnicas. NBR 11941: madeira - determinação da densidade básica. Rio de Janeiro, 2003, 6p.

ALVES, M. C. S.; SILVA, T. A.; TONETTI, O. A. O.; et al. Use of near infrared spectroscopy for estimating moisture content in Brazilian cherry (*Eugenia uniflora* L.) seeds submitted to dehydration clones. CERNE, v. 30, n.1, e-103414, 2024. https://doi.org/10.1590/01047760202330013414.

ARAÚJO, A. C. C.; COSTA, L. J.; BRAGA, P. P. C.; et al. Propriedades energéticas da madeira e do carvão vegetal de *Cenostigma macrophyllum*: subsídios ao uso sustentável. Pesquisa Florestal Brasileira, v. 38, n. 2018, p. 1-9, 2018. https://doi.org/10.4336/2018.pfb.38e201701546.

ASSIS, M. R.; BRANCHERIAU, L.; NAPOLI, A.; et al. Factors affecting the mechanics of carbonized wood: literature review. Wood Science and Technology, v. 50, n. 2016, p. 519-536, 2016. https://doi.org/10.1007/s00226-016-0812-6.

COSTA, A. C. P. R.; RAMALHO, F. M. G.; RIBEIRO, L. C.; et al. Classification of commercial charcoal for domestic use by near infrared spectroscopy. Biomass and Bioenergy, v. 127, p. 105280, 2019. https://doi.org/10.1016/j.biombioe.2019.105280.

COSTA, L. J.; TRUGILHO, P. F.; LIMA, J. T.; et al. Mechanic characterization of charcoal of *Corymbia* clones. Scientia Forestalis, v. 45, p. 629–639, 2017. https://doi.org/10.18671/scifor.v45n116.04.

COSTA, L. R.; TRUGILHO, P. F.; HEIN, P. R. G. Evaluation and classification of eucalypt charcoal quality by near infrared spectroscopy. Biomass and Bioenergy, v. 112, p. 85-92, 2018. https://doi.org/10.1016/j.biombioe.2018.02.017.

COUTO, A. M.; MONTEIRO, T. C.; TRUGILHO, P. F.; et al. Influence of physical-anatomical wood variables on charcoal physical–mechanical properties. Journal of Forestry Research, v. 34, p. 531–538, 2023. https://doi.org/10.1007/s11676-022-01462-9.

COUTO, A. M.; TRUGILHO, P. F.; NAPOILI, A.; et al. Quality of charcoal from *Corymbia* and *Eucalyptus* produced at different final carbonization temperatures. Scientia Forestalis, v. 43, p. 817-831, 2015.https://doi.org/10.18671/scifor.v43n108.7.

DIAS JÚNIOR, A. F.; OLIVEIRA, R. N.; DEGLISE, X.; et al. Infrared spectroscopy analysis on charcoal generated by the pyrolysis of *Corymbia citriodora* wood. Matéria (Rio de Janeiro), v. 24, p. e12387, 2019. https://doi.org/10.1590/S1517-707620190003.0700.

EPE – Empresa de Pesquisa Energética. Balanço energético nacional 2024: ano base 2023. Rio de Janeiro: EPE, 2024, 70p.

FORTALEZA, A. P.; NASCIMENTO FILHO, J. J. P.; CERETTA, R. P. S. Biomassa de espécies florestais para produção de carvão vegetal. Ciência Florestal, v. 29, n. 3, p. 1436-1451, 2019. https://doi.org/10.5902/1980509831639.

GMACH, F.; ARRUDA, L. J.; BONFATTI JÚNIOR, E. A.; et al. Performance of visible and Near-infrared spectroscopy to predict the energetic properties of wood. Maderas. Ciencia y Tecnología, v. 26, p. 1-14, 2024. https://doi.org/10.22320/s0718221x/2024.11.

GOMES, J. N. N.; MEDEIROS, D. T.; COLARES, C. J. G.; et al. Estimation of energy properties of wood from Brazilian Cerrado biome by NIR spectroscopy. Journal of the Indian Academy of Wood Science, v. 21, n. 2, p. 306-315, 2024. https://doi.org/10.1007/s13196-024-00349-y.

HEIN, P. R. G.; LIMA, J. T.; CHAIX, G. Effects of sample preparation on NIR spectroscopic estimation of chemical properties of *Eucalyptus urophylla* S.T. Blake wood. Holzforschung, v. 64, n. 1, p. 45-54, 2010. https://doi.org/10.1515/hf.2010.011.

JO, T. S.; LEE, O. K.; CHOI, J. W.; et al. Changes of chemical bond in woody charcoal from different carbonization temperatures. Journal of the Korean Wood Science and Technology, v. 37, p. 87-93, 2009.

LIMA, M. D. R.; BUFALINO, L.; SCATOLINO, M. V.; et al. Segregating Amazonia logging wastes from sustainable forest management improves carbonization in brick kilns. Renewable Energy, v. 211, p. 772-788, 2023. https://doi.org/10.1016/j.renene.2023.04.126.

LIMA, M. D. R.; PATRÍCIO, E. P. S.; BARROS JÚNIOR, U. O; et al. Logging wastes from sustainable forest management as alternative fuels for thermochemical conversion systems in Brazilian Amazon. Biomass and Bioenergy, v. 140, p. 105660, 2020. https://doi.org/10.1016/j.biombioe.2020.105660.

LIMA, M. D. R.; MASSUQUE, J.; BUFALINO, L.; et al. Clarifying the carbonization temperature effects on the production and apparent density of charcoal derived from Amazonia wood wastes. Journal of Analytical and Applied Pyrolysis, v. 166, p. 105636, 2022a. https://doi.org/10.1016/j.jaap.2022.105636.

LIMA, M. D. R.; TRUGILHO, P. F.; BUFALINO, L.; et al. Efficiency of near-infrared spectroscopy in classifying Amazonian wood wastes for bioenergy generation. Biomass and Bioenergy, v. 166, p. 106617, 2022b. https://doi.org/10.1016/j.biombioe.2022.106617.

LIU, Z.; NIU, W.; CHU, H.; et al. Effect of the carbonization temperature on the properties of biochar produced from the pyrolysis of crop residues. BioResources, v. 13, n. 2, p. 3429-3446, 2018. https://doi.org/10.15376/biores.13.2.3429-3446.

LOUREIRO, B. A.; ARRIEL, T. G.; RAMALHO, F. M. G.; et al. NIR-based models for estimating selected physical and chemical wood properties from fast-growing plantations. iForest, v. 15, p. 372-380, 2022. https://doi.org/10.3832/ifor4030-015.

LOUREIRO, B. A.; ASSIS, M. R.; MELO, I. C. N. A. Rendimento gravimétrico da carbonização e caracterização qualitativa do carvão vegetal em clones de híbridos de *Corymbia* spp para uso industrial. Ciência Florestal, v. 31, n. 1, p. 214-232, 2021. https://doi.org/10.5902/1980509836120.

MACHADO, G. O.; VOGEL, F.; MORAES, M. Influência da temperatura final de carbonização nas características físicas, químicas e energéticas do carvão de cinamomo (*Melia azedarach* L.). Ambiência, v. 10, n. 1, p. 83-96, 2014. https://doi.org/10.5935/ambiencia.2014.01.07.

MEDEIROS, D. T.; MELO, R. R.; CADEMARTORI, P. H. G.; et al. Prediction of the basic density of tropical woods by near-infrared spectroscopy. CERNE, v.29, e-103262, 2023. https://doi.org/10.1590/01047760202329013262.

MUÑIZ, G. I. B.; CARNEIRO, M. E.; NISGOSKI, S.; et al. SEM and NIR characterization of four forest species charcoal. Wood Science and Technology, v. 47, p. 815-823, 2013. https://doi.org/10.1007/s00226-013-0539-6.

NASCIMENTO, C. C.; BRASIL, M. M.; NASCIMENTO, C. S.; et al. Estimativa da densidade básica da madeira de *Eschweilera odora* (Poepp.) Miers por espectroscopia no infravermelho próximo. Ciência da Madeira, v. 8, n. 1, p. 42-53, 2017. https://doi.org/10.12953/2177-6830/rcm.v8n1p42-53.

NUNES, C. A.; FREITAS, M. P.; PINHEIRO, A. C. M. Chemoface: a novel free user-friendly interface for chemometrics. Journal of the Brazilian Chemical Society, v. 23, n. 11, p. 2003-2010, 2012. https://doi.org/10.1590/S0103-50532012005000073.

OLIVEIRA, A. C.; RAMOS, D. C.; PEREIRA, B. L. C.; et al. Carbonization temperature and charcoal properties at different positions in rectangular kiln. Revista Brasileira de Ciências Agrárias, v. 15, n. 4, p. 1-8, 2020. https://doi.org/10.5039/agraria.v15i4a8493.

PINTO, R. G. D.; SZKLO, A. S.; RATHMANN, R. CO_2 emissions mitigation strategy in the Brazilian iron and steel sector – From structural to intensity effects. Energy Policy, v. 114, p. 380-393, 2018. https://doi.org/10.1016/j.enpol.2017.11.040.

RECH, Â. F.; WERNER, S. S. Utilização da espectroscopia no infravermelho próximo e calibração multivariada para determinação da composição nutricional de azevém. Agropecuária Catarinense, v. 37, n. 1, p. 55-62, 2024. https://doi.org/10.52945/rac.v37i1.1781.

SANTOS, V. B.; BARAÚNA, E. E. P.; COLEN, F.; et al. Energy characterization of wood and charcoal from Savannah forest species. BioResources, v. 18, n. 1, p. 1780, 2023. https://doi.org/10.15376/biores.18.1.1780-1787.

SANTOS, L. M.; AMARAL, E. A.; NIERI, E. M.; et al. Estimating wood moisture by near infrared spectroscopy: testing acquisition methods and wood surfaces qualities. Wood Material Science & Engineering, v. 16, p. 336-343, 2021. https://doi.org/10.1080/17480272.2020.1768143.

SCHIMLECK, L. R.; MATOS, J. L. M.; TRIANOSKI, R.; et al. Comparison of methods for estimating mechanical properties of wood by NIR spectroscopy. Journal of Spectroscopy, v. 2018, p. 4823285, 2018. https://doi.org/10.1155/2018/4823285.

SILVA, A. A.; SOUSA, K. C.; SOUZA, F. I. B.; et al. Forestry control in the Brazilian Amazon III: anatomy of wood and charcoal of tree species from sustainable forest management. IAWA Journal, v. 45, n. 3, p. 297–334, 2024. https://doi.org/10.1163/22941932-bja10151.

SILVA, L. F. F.; CASTRO, A. R. S.; OLIVEIRA, R. S.; et al. Seleção de espécie, temperatura e tempo de carbonização na produção de carvão vegetal com resíduos madeireiros da Amazônia. Pesquisa Florestal Brasileira, v. 40, p. 1-11, 2020. https://doi.org/10.4336/2020.pfb.40e201801737.

SINDIFER – Sindicato da Industria do Ferro no Estado de Minas Gerais. Anuário estatístico 2023, ano base 2022: produção de ferro-gusa em Minas Gerais e no Brasil, 2023.

TRUGILHO, P. F.; SILVA, D. A. Influence of final carbonization temperature in the physical and chemical characteristics of the jatoba (*Himenea courbaril* L.) charcoal. Scientia Agraria, v. 2, p. 1–8, 2001. https://doi.org/10.5380/rsa.v2i1.976.

TRUGILHO, P. F.; SILVA, D. A.; FRAZÃO, F. J. L.; et al. Caracterização de espécies nativas e exóticas amazônicas e do carvão vegetal. Revista Árvore, v. 15, n. 2, p. 144-151, 1991.

WU, X.-F.; LI, S.-X.; LI, M.-F. Effect of temperature on the properties of charcoal prepared from carbonization of biorefinery lignin. Bioresources, v. 13, n. 3, p. 6736-6745, 2018. https://doi.org/10.15376/biores.13.3.6736-6745.